CaliGCL: Calibrated Graph Contrastive Learning via Partitioned Similarity and Consistency Discrimination

Yuena Lin [1,†], Hao Wei [1,†], Haichun Cai [2], Bohang Sun [1], Tao Yang [3], Zhen Yang [1], & Gengyu Lyu [1,*]
[1] College of Computer Science, Beijing University of Technology, Beijing
[2] College of Computer and Data Science, Fuzhou University, Fuzhou
[3] Idealism Beijing Technology Co., Ltd., Beijing
yuenalin@126.com, haowei@emails.bjut.edu.cn, fjsmchc@163.com
sunbohang@bjut.edu.cn, yangtao@ilxzy.cn, yangzhen@bjut.edu.cn
lyugengyu@gmail.com

Abstract

Graph contrastive learning (GCL) aims to learn self-supervised representations by distinguishing positive and negative sample pairs generated from multiple augmented graph views. Despite showing promising performance, GCL still suffers from two critical biases: (1) **Similarity estimation bias** arises when feature elements that support positive pair alignment are suppressed by conflicting components within the representation, causing truly positive pairs to appear less similar. (2) **Semantic shift bias** occurs when random augmentations alter the underlying semantics of samples, leading to incorrect positive or negative assignments and injecting noise into training. To address these issues, we propose CaliGCL, a GCL model for calibrating the biases by integrating an exponential partitioned similarity measure and a semantics-consistency discriminator. The exponential partitioned similarity computes the similarities among fine-grained partitions obtained through splitting representation vectors and uses exponential scaling to emphasize aligned (positive) partitions while reducing the influence of misaligned (negative) ones. The discriminator dynamically identifies whether augmented sample pairs maintain semantic consistency, enabling correction of misleading contrastive supervision signals. These components jointly reduce biases in similarity estimation and sample pairing, guiding the encoder to learn more robust and semantically meaningful representations. Extensive experiments on multiple benchmarks show that CaliGCL effectively mitigates both types of biases and achieves state-of-the-art performance.

1 Introduction

General graph contrastive learning (GCL) follows a pipeline to realize self-supervised representation learning [1, 2, 3], which includes: implement augmentations on raw data to generate multiple views [4], encode the augmented data to produce representations [5], and finally adopt a common contrastive supervision that corresponding samples across different augmented views are positives while others are negatives for contrastive learning [6, 7, 8]. Even though this GCL framework is well recognized, it still incurs **similarity estimation bias** and **semantic shift bias**, which may degrade the graph encoder to generate inferior representations.

The similarity estimation bias arises from the fact that representations produced by the encoder are typically composed of conflicting positively- and negatively-synergistic feature elements, where the

*Corresponding author, † equal contributions.

39th Conference on Neural Information Processing Systems (NeurIPS 2025).

positively-synergistic feature elements are those for supporting the alignment of latent positive pairs within representation vectors, while the negatively-synergistic feature elements are those that work against the positively-synergistic ones. When computing the similarity (commonly via inner product) between two representations, these conflicting feature elements would cancel each other out even within positive pairs. This undermines the model ability to identify the latent positive pairs, leading to suboptimal representation learning.

To illustrate how negatively-synergistic features suppress similarity, we conduct a statistical analysis on the ratio between positively-aligned and negatively-aligned partitions under different partition settings in Figure 1, where a partition is positively-aligned if the corresponding feature elements have the positive inner product, otherwise negatively-aligned. Each partition refers to a subset of feature elements within a representation. In the experiment, we follow the GCL framework to train an encoder on Citeseer dataset and divide the generated representations into multiple partitions. With label guidance, we calculate the ratios of positively- and negatively-aligned partitions within positive sample pairs. As the number of partitions increases, the ratio of negatively-aligned partitions grows, revealing the prevalence of conflicting feature elements in the learned representations. This trend suggests that *when computing overall similarity via inner product, multiple negatively-aligned partitions collectively suppress positively-aligned ones, ultimately leading to the similarity estimation bias*.

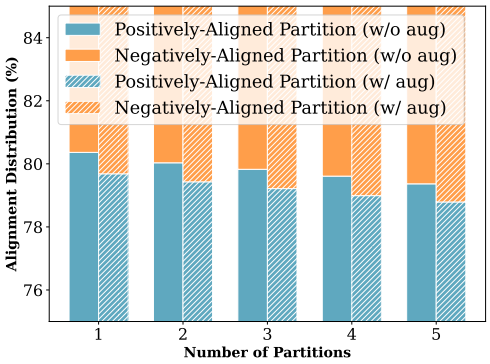

Figure 1: Ratio (alignment distribution) of positively-aligned to negatively-aligned similarity partitions under different partition settings. Shaded histogram bars represent results obtained with graph augmentations, while unshaded ones denote results without augmentations.

Apart from the similarity estimation bias, random graph augmentations in GCL easily flip the relationship between sample pairs, which would result in semantic shift bias. Specifically, graph augmentations as common tools in GCL [9, 10] may alter essential node features or graph topology [11, 12], which potentially flips the relationship between sample pairs: semantically consistent sample pairs may be assigned as negatives, while semantically divergent ones may be incorrectly treated as positives [13]. This introduces noise into contrastive supervision and misguides the training process [14, 15]. Figure 1 illustrates this problem under the condition where the number of partitions is only 1, and the inner product of the partition is equivalent to the inner product of two representation vectors. It could be found that the ratios change when comparing the alignment distributions with and without augmentations, which suggests that augmentations possibly flip the nature of sample pairs (positive $\leftrightarrow$ negative). Importantly, *when these flipped pairs are treated as fixed positives or negatives under conventional contrastive supervision, the error will propagate through the training process, causing the encoder to become biased due to semantic shift*.

To calibrate the biases in GCL, we propose a novel graph contrastive model CaliGCL, which integrates an exponential partitioned similarity measure and a semantics-consistency discriminator. The exponential partitioned similarity measure first splits each representation vector into fine-grained partitions and computes the inner product similarity among each partition, then applies an exponential function to shrink the negatively-aligned partition similarities while amplifying the positively-aligned partition similarities, thereby improving the influence of positively-synergistic feature elements and reducing the suppression of negatively-synergistic feature elements to alleviate the similarity estimation bias. The semantics-consistency discriminator [16, 17] takes the sample pair information as input and dynamically predicts relationship consistency scores after augmentation, which are used for calibrating the contrastive supervision to enhance the resilience of GCL and combat semantic shift bias. The two components cooperate to realize debiased GCL and guide the encoder to learn more robust and semantically meaningful representations. Our contributions are summarized as follows:

- We identify two critical biases in the standard GCL framework, namely similarity estimation bias and semantic shift bias, and propose a novel calibrated graph contrastive learning model, CaliGCL, to systematically address them.

- We propose an exponential partitioned similarity measure to restrict the negatively-synergistic features and amplify the positively-synergistic features to alleviate the similarity estimation bias. Besides, a semantics-consistency discriminator is proposed to correct the semantic relationships of augmented sample pairs, effectively debiasing semantic shift.
- Extensive experiments across multiple datasets show that the proposed model consistently surpasses advanced self-supervised graph models, which demonstrate that our model effectively calibrates the biases in GCL and enhances the representation quality.

2 Related works

Problem definition and notations. In this paper, a graph is denoted as $\mathcal{G} = (\mathcal{V}, \mathcal{E})$, where $\mathcal{V} = \{v_1, v_2, \cdots, v_N\}$ is the node set with N nodes and $\mathcal{E} \subset \mathcal{V} \times \mathcal{V}$ is the edge set. The node attribute matrix and adjacency matrix are denoted as $\boldsymbol{X} \in \mathbb{R}^{N \times F}$ and $\boldsymbol{A} \in \{0,1\}^{N \times N}$, respectively. We aim to train an L-layer graph encoder $f : \mathbb{R}^{N \times F} \times \{0,1\}^{N \times N} \to \mathbb{R}^{N \times d}$ to produce low-dimensional node representations via raw attribute and structure contents [18], where d is the dimension of the L-th layer, and F is the dimension of the raw attribute.

Graph neural networks. Graph neural networks (GNNs) have been widely adopted for learning graph data by recursively aggregating and combining information from the local neighborhoods to generate expressive node- or graph-level representations [19, 20]. Each layer in a GNN follows the message-passing mechanism, always including `AGGREGATE` and `COMBINE` two stages. Given a graph $\mathcal{G}$, the output $\boldsymbol{h}_v^{(l)}$ of l-th GNN layer is defined as:

$$\boldsymbol{m}_v^{(l)} = \texttt{AGGREGATE}\left(\{\boldsymbol{h}_u^{(l-1)} : u \in \mathcal{N}(v)\}\right), \ \boldsymbol{h}_v^{(l)} = \texttt{COMBINE}\left(\boldsymbol{h}_v^{(l-1)}, \boldsymbol{m}_v^{(l)}\right), \tag{1}$$

where $\boldsymbol{h}_v^{(l)}$ is the representation of v at l-th layer, and $\mathcal{N}(v)$ denotes its neighbors. The `AGGREGATE` stage gathers neighbor information and outputs aggregated information $\boldsymbol{m}_v^{(l)}$, while the `COMBINE` stage integrates it with the self-information $\boldsymbol{h}_v^{(l-1)}$. A graph-level representation is derived with `READOUT` function [21]:

$$\boldsymbol{h}_{\mathcal{G}} = \texttt{READOUT}\left(\{\mathbf{h}_v^{(l)} : v \in \mathcal{V}\}\right). \tag{2}$$

Graph contrastive learning. A typical GCL framework begins by implementing two augmentation functions $\mathcal{T}_U$ and $\mathcal{T}_V$ on the input graph $\mathcal{G} = (\boldsymbol{X}, \boldsymbol{A})$ to obtain two augmented views $U = \mathcal{T}_U(\mathcal{G})$ and $V = \mathcal{T}_V(\mathcal{G})$. These augmented graphs are processed by a GNN encoder $f(\cdot)$ to generate representations $\boldsymbol{H}_U = f(U)$ and $\boldsymbol{H}_V = f(V)$.

To train the model, a contrastive objective follows the contrastive supervision that the corresponding samples in the two views are positive, while other samples are negative. For a sample pair (u_i, v_i), the contrastive loss based on the InfoNCE principle [22] is defined as:

$$\ell_{ct}(\boldsymbol{h}_{u_i}, \boldsymbol{h}_{v_i}) = -\log \frac{\exp\left(\mathcal{S}(\boldsymbol{h}_{u_i}, \boldsymbol{h}_{v_i})/\tau\right)}{\sum_j \exp\left(\mathcal{S}(\boldsymbol{h}_{u_i}, \boldsymbol{h}_{v_j})/\tau\right) + \sum_{j \neq i} \exp\left(\mathcal{S}(\boldsymbol{h}_{u_i}, \boldsymbol{h}_{u_j})/\tau\right)}, \tag{3}$$

where $\mathcal{S}(\cdot, \cdot)$ denotes a similarity function, and τ is a temperature coefficient. The overall objective sums the contrastive losses over all nodes:

$$\mathcal{L}_{ct} = \frac{1}{2N} \sum_{i=1}^{N} \left(\ell_{ct}(\boldsymbol{h}_{u_i}, \boldsymbol{h}_{v_i}) + \ell_{ct}(\boldsymbol{h}_{v_i}, \boldsymbol{h}_{u_i})\right). \tag{4}$$

Though this simple-yet-effective idea that maximizes the mutual information [23] is followed by considerable works [24, 25], recent studies have raised concerns regarding the rationality of contrastive supervision, particularly in how positive and negative samples are selected. NCLA [26] notices the fact that neighboring nodes are viewed as negatives is contradictory with the homophily principle, and introduces a neighbor contrastive loss to include additional positives. HomoGCL [27] finds that a part of connected nodes belonging to different classes would degrade the model performance when treating them as positives, then leverages a Gaussian mixture model to calculate the sample similarities for assigning weights to potential positives. While these methods have made important

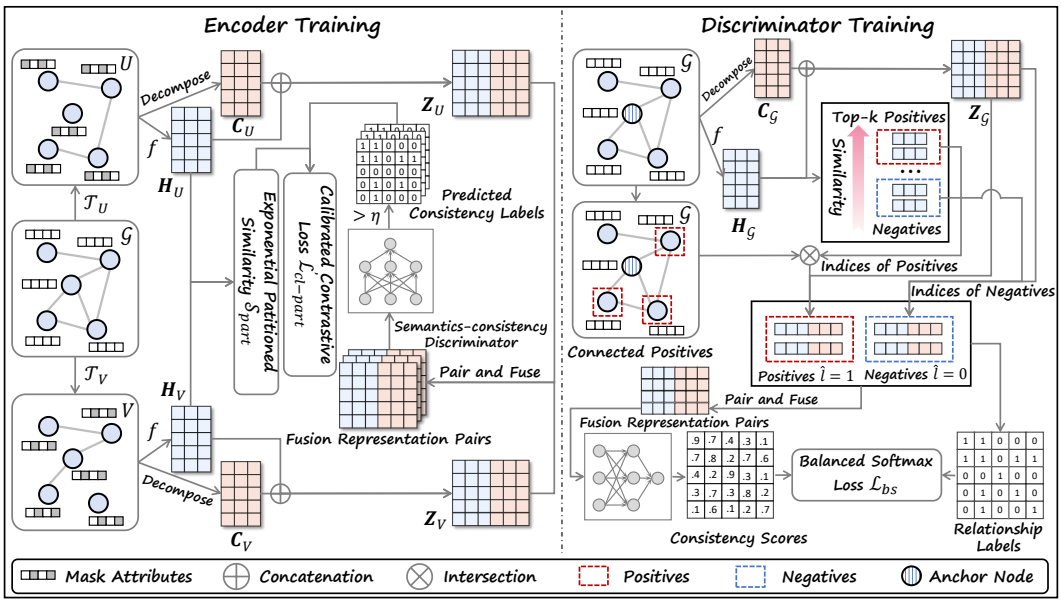

Figure 2: Training process for ClaiGCL. During encoder training, input graph $\mathcal{G}$ is transformed as views U and V with augmentations $\mathcal{T}_U$ and $\mathcal{T}_V$ to abstract feature information $\boldsymbol{H}_U$ and $\boldsymbol{H}_V$, and structure information $\boldsymbol{C}_U$ and $\boldsymbol{C}_V$ for constructing fusion representations $\boldsymbol{Z}_U$ and $\boldsymbol{Z}_V$. The fusion representations are constructed as inter-view and intra-view pairs that are then fused and input into the semantics-consistency discriminator to predict the relationship labels for calibrating the contrastive loss. During discriminator training, $\mathcal{G}$ is used to abstract feature information $\boldsymbol{H}_\mathcal{G}$ and structure information $\boldsymbol{C}_\mathcal{G}$ for constructing the fusion representation $\boldsymbol{Z}_\mathcal{G}$, where $\boldsymbol{H}_\mathcal{G}$ is also employed to select positives and negatives as pre-defined relationship labels with the k-NN algorithm and the homophily principle (i.e., connected positives). The positives and negatives are selected from $\boldsymbol{Z}_\mathcal{G}$ with corresponding indices, which are input into the discriminator for obtaining the consistency scores for calculating balanced softmax loss along with the relationship labels.

strides in refining contrastive supervision, most of them primarily focus on local neighborhood relationships. In contrast, our proposed CaliGCL expects to calibrate the wrong relationships from a global view, which offers a principled solution to reduce similarity estimation bias and semantic shift bias beyond local structural corrections.

3 CaliGCL

The training process of CaliGCL includes encoder training and discriminator training. When training the encoder, CaliGCL implements the exponential partitioned similarity measure into the contrastive loss to relieve the conflicts between positively- and negatively-synergistic features. Besides, it introduces a semantics-consistency discriminator to calibrate the semantic shift bias caused by the fixed contrastive supervision in GCL. Figure 2 shows the overview of both training processes.

3.1 Exponential partitioned similarity measure

When gauging the similarity of a positive pair, the positively-synergistic feature elements dominate to capture semantic consistency. However, the representation vectors are always composed of both positively- and negatively-synergistic feature elements, which easily cause conflicts in similarity calculation and obscure the semantic relationships between sample pairs.

Theorem 1 *Given a positive representation pair $(\boldsymbol{h}_u, \boldsymbol{h}_v)$ with d feature elements, where each element of $\boldsymbol{h}_u$ and $\boldsymbol{h}_v$ is independent and identically distributed (i.i.d.) following a normal distribution $\mathcal{N}(\mu, \sigma^2)$. Suppose that the expectation of the inner product of $\boldsymbol{h}_u$ and $\boldsymbol{h}_v$ is a positive value M, then for a partition consisting of m $(m \leq d)$ features, the probability that the inner product over*

this partition is a negative value is $\Phi\left(\frac{-m\mu^2}{\sqrt{m(\mu^2+2\sigma^2)^2}}\right)$*, where* $\Phi(\cdot)$ *is the cumulative distribution function of the standard normal distribution.*

This theorem provides the possibility that negatively-synergistic features exist in a positive pair. To address this, we introduce an exponential partitioned similarity measure, specifically designed to reduce the impairments of negatively-synergistic feature elements while enhancing the influence of positively-synergistic ones, thereby mitigating the conflicts between the two types of features and strengthening semantic alignment in representation learning.

In our design, a representation is split into K fine-grained partitions, with each containing a subset of the feature elements. Thus, for the representation $\boldsymbol{h}_{v_i} = f(v_i) \in \mathbb{R}^d$ of node v_i, it can be represented as $\boldsymbol{h}_{v_i} = [\boldsymbol{h}_{v_i}^{(1)} \parallel \boldsymbol{h}_{v_i}^{(2)} \parallel \cdots \parallel \boldsymbol{h}_{v_i}^{(K)}]$, where $\parallel$ is the concatenation operator, and $\{\boldsymbol{h}_{v_i}^{(k)}\}_{k=1}^{K}$ represents the different partitions of $\boldsymbol{h}_{v_i}$. Among these partitions, each of the first $(K-1)$ partitions contains m feature elements, and the last partition has $d-(K-1)m$ feature elements, where m is a hyperparameter to control the partition size.

We use $\mathcal{S}_{part}(\boldsymbol{h}_{v_i}, \boldsymbol{h}_{v_j})$ to represent the exponential partitioned similarity between a sample pair (v_i, v_j), which is mathematically defined as the sum of inner product similarity over K partitions:

$$\mathcal{S}_{part}(\boldsymbol{h}_{v_i}, \boldsymbol{h}_{v_j}) = \frac{1}{K}\sum_{k=1}^{K} \exp\left(\frac{K \cdot \boldsymbol{h}_{v_i}^{(k)\top}\boldsymbol{h}_{v_j}^{(k)}}{\tau}\right), \tag{5}$$

where τ is the temperature coefficient. Unlike the commonly-used exponential inner product in contrastive learning, i.e., $\exp(\boldsymbol{h}_{v_i}^{\top}\boldsymbol{h}_{v_j}/\tau)$, our method computes the inner product for each partition independently before applying the exponential sum on the results. This design naturally suppresses the impact of negatively-aligned partitions by inducing their exponentials to approach zero while amplifying positively-aligned ones. For instance, given a positive pair (v_i, v_j) having positive inner product is divided into two partitions where the first is negatively-aligned and the second positively-aligned, it is easy to find the following conclusion:

$$\exp\left(\frac{2 \cdot \boldsymbol{h}_{v_i}^{(1)\top}\boldsymbol{h}_{v_j}^{(1)}}{\tau}\right) \to 0, \; \textit{and} \;\; \exp\left(\frac{2 \cdot \boldsymbol{h}_{v_i}^{(2)\top}\boldsymbol{h}_{v_j}^{(2)}}{\tau}\right) \geq \exp\left(\frac{\boldsymbol{h}_{v_i}^{\top}\boldsymbol{h}_{v_j}}{\tau}\right). \tag{6}$$

This holds since $\boldsymbol{h}_{v_i}^{\top}\boldsymbol{h}_{v_j} = \boldsymbol{h}_{v_i}^{(1)\top}\boldsymbol{h}_{v_j}^{(1)} + \boldsymbol{h}_{v_i}^{(2)\top}\boldsymbol{h}_{v_j}^{(2)}$ and $\boldsymbol{h}_{v_i}^{(2)\top}\boldsymbol{h}_{v_j}^{(2)} > \boldsymbol{h}_{v_i}^{\top}\boldsymbol{h}_{v_j}$ Thus, the overall partitioned similarity is more influenced by positively-synergistic components. Furthermore, we provide the following theorem to explain that the proposed exponential partitioned similarity is larger than the standard exponential inner product across all scenarios.

Theorem 2 *The exponential partitioned similarity provides an upper bound on the standard exponential inner product similarity between two representations.*

This similarity measure will be used in the contrastive loss for debiasing the similarity conflicts.

3.2 Semantics-consistency discriminator

During the contrastive training, random augmentations may flip the semantic consistency between sample pairs, which implies that positive and negative sample pairs convert to each other potentially. This is difficult to perceive with the fixed contrastive supervision that the corresponding samples across different augmented views are positives, while others are negatives. To alleviate the harm from the strong assumption, we propose a semantics-consistency discriminator to dynamically evaluate the semantic relationships among sample pairs during the training process. The discrimination process includes two parts: (1) feature and structure encoding, and (2) semantics-consistency discrimination.

Feature and structure encoding. To provide sufficient pair information to support semantics-consistency judgements, we incorporate both feature and structural information as the input for the discriminator. For a sample pair (v_i, v_j), we employ a GNN encoder to generate the corresponding representation pair $(\boldsymbol{h}_{v_i}, \boldsymbol{h}_{v_j})$ as the feature information. Meanwhile, we decompose the graph Laplacian matrix to obtain the eigenvectors as node structural information [28], which is defined as:

$$\tilde{\boldsymbol{A}} = \boldsymbol{U}\boldsymbol{\Lambda}\boldsymbol{U}^{\top}. \tag{7}$$

$\tilde{\boldsymbol{A}}$ is the normalized adjacency matrix as [29], and it is defined as $\tilde{\boldsymbol{A}} = \hat{\boldsymbol{D}}^{-\frac{1}{2}}\hat{\boldsymbol{A}}\hat{\boldsymbol{D}}^{-\frac{1}{2}}$, where $\hat{\boldsymbol{A}} = \boldsymbol{A} + \boldsymbol{I}_N$, $\hat{\boldsymbol{D}}$ is a diagonal matrix, and its diagonal element is $\hat{\boldsymbol{D}}_{ii} = \sum_j \hat{\boldsymbol{A}}_{ij}$. $\boldsymbol{U}$ is an orthogonal matrix constructed with eigenvectors, and $\boldsymbol{\Lambda}$ is a diagonal matrix filled with eigenvalues. We select t eigenvectors corresponding to top-t greatest eigenvalues as the final node structure embeddings, which is denoted as $\boldsymbol{C} \in \mathbb{R}^{N\times t}$, and denote the structure embeddings for v_i and v_j as $\boldsymbol{c}_{v_i}$ and $\boldsymbol{c}_{v_j}$, respectively.

Semantics-consistency discrimination. In this process, the feature encoding $(\boldsymbol{h}_{v_i}, \boldsymbol{h}_{v_j})$ and structural encoding $(\boldsymbol{c}_{v_i}, \boldsymbol{c}_{v_j})$ are concatenated to form a new fusion representation pair as $\left(\boldsymbol{z}_{v_i} = \boldsymbol{h}_{v_i} \parallel \boldsymbol{c}_{v_i}, \boldsymbol{z}_{v_j} = \boldsymbol{h}_{v_j} \parallel \boldsymbol{c}_{v_j}\right)$. Then the representation pair $(\boldsymbol{z}_{v_i}, \boldsymbol{z}_{v_j})$ containing both the feature and structural information is used for evaluating the semantic consistency. Specifically, the representation pair $(\boldsymbol{z}_{v_i}, \boldsymbol{z}_{v_j})$ is first fused and then input into the semantics-consistency discriminator $D(\cdot)$ that is defined as a multi-layer perceptron (MLP) with a non-linear activation function. The process is defined as:

$$p_{v_i,v_j} = D(\boldsymbol{z}_{v_i} \odot \boldsymbol{z}_{v_j}), \tag{8}$$

where the Hadamard product $\odot$ is used to fuse $\boldsymbol{z}_{v_i}$ and $\boldsymbol{z}_{v_j}$, p_{v_i,v_j} is the predicted consistency score of pair $(\boldsymbol{z}_{v_i}, \boldsymbol{z}_{v_j})$ by the discriminator. Finally, p_{v_i,v_j} is used to judge the semantic relationship between v_i and v_j according to the following rule:

$$\tilde{l}_{v_i,v_j} = \begin{cases} 1, & \text{if } p_{v_i,v_j} \geq \eta \\ 0, & \text{if } p_{v_i,v_j} < \eta \end{cases}, \tag{9}$$

where η is the threshold. $\tilde{l}_{v_i,v_j}$ is defined as the predicted consistency label, where $\tilde{l}_{v_i,v_j} = 1$ means the pair (v_i, v_j) is positive, and $\tilde{l}_{v_i,v_j} = 0$ denotes the pair is negative. This label is critical for recognizing the varying relationships of sample pairs.

3.3 Training strategy for CaliGCL

Training overview. The training strategy for CaliGCL is composed of a pre-training process and a fine-tuning process. The pre-training process trains the GNN encoder to produce similarity-debiased representations by integrating the exponential partitioned similarity into the contrastive learning and develops the ability of the semantics-consistency discriminator for capturing the changing semantics of sample pairs. The fine-tuning process adopts an alternating algorithm: the discriminator is employed to calibrate the contrastive loss by correcting false positive or negative sample pair assignments caused by augmentation-induced semantic flips. Then the calibrated encoder generates more reliable representations to further enhance the discriminator in distinguishing the semantics-consistency relationships. The training strategy for improving both representation quality and semantic discrimination is detailed in the following.

3.3.1 Pre-training process

Pre-training for similarity-debiased GNN. Following the standard GCL paradigm, we implement the augmentations on the raw graph to generate two augmented graphs U and V, where each node $u_i \in U$ and its counterpart $v_i \in V$ form a positive pair, while others are negatives. The key difference in our framework lies in replacing the exponential inner product similarity function with the proposed exponential partitioned similarity in the contrastive loss, which is called the partitioned contrastive loss here. And the partitioned contrastive loss for u_i is defined as

$$\ell_{cl-part}(u_i) = -\log \frac{\mathcal{S}_{part}(\boldsymbol{h}_{u_i}, \boldsymbol{h}_{v_i})}{\sum_j \mathcal{S}_{part}(\boldsymbol{h}_{u_i}, \boldsymbol{h}_{v_j}) + \sum_{j\neq i} \mathcal{S}_{part}(\boldsymbol{h}_{u_i}, \boldsymbol{h}_{u_j})}, \tag{10}$$

To ensure sufficient interactions among feature dimensions across partitions, we shuffle the feature columns of representations before loss computation. And the overall loss is given by:

$$\mathcal{L}_{cl-part} = \frac{1}{2N}\sum_{i=1}^{N}\left[\ell_{ct-part}(u_i) + \ell_{ct-part}(v_i)\right]. \tag{11}$$

Theorem 3 *Assume the similarity of each partition for positive pairs $\mathcal{S}^+_{part}$ obeys $\mathcal{N}(\mu_1, \sigma_1^2)$, and the similarity of each partition for negative pairs $\mathcal{S}^-_{part}$ obeys $\mathcal{N}(\mu_2, \sigma_2^2)$. If $\sigma_1^2 > \sigma_2^2$ and the partition*

similarities are i.i.d., then the partitioned contrastive objective serves as a tighter lower bound on mutual information, and yields an upper-bounded estimate compared with the contrastive objective.

The assumption that $\sigma_1^2 \geq \sigma_2^2$ is reasonable based on the fact that the positive samples are similar because of the existence of positively-synergistic feature elements, while other negatively-synergistic feature elements would cause great divergence. In contrast, negative pairs tend to be uniformly dissimilar, leading to lower overall variance in their feature alignment. This variance divergence across partitions results in a sharper separation under exponential partitioned similarity, thus achieving a more ideal contrastive objective.

Pre-training for semantics-consistency discriminator. The key to training the discriminator depends on adopting reliable positive and negative pairs with pre-defined relationship labels. Specifically, a sample pair (v_i, v_j) is assigned a positive relationship label $\hat{l}_{v_i,v_j} = 1$ only if the samples are both directly connected (topology proximity) and k-NN neighbors (feature closeness). Otherwise, we assign $\hat{l}_{v_i,v_j} = 0$ and treat the pairs as negative. Since the pre-trained GNN encoder still suffers from the semantic shift bias, the k-NN algorithm is applied in the original feature space but not the representation space.

Let N_{pos} and N_{neg} denote the total number of pre-defined positive and negative pairs, respectively. Due to $N_{pos} \ll N_{neg}$ in general, the imbalance leads the discriminator to overly favor negative predictions. Thus, we employ the Balanced Softmax loss [30, 31] to mitigate the imbalance problem:

$$\mathcal{L}_{bs} = -\sum_{i,j} \log \frac{\mathbb{I}(\hat{l}_{v_i,v_j} = 1) \exp(p_{v_i,v_j} + \log N_{pos}) + \mathbb{I}(\hat{l}_{v_i,v_j} = 0) \exp(p_{v_i,v_j} + \log N_{neg})}{\exp(p_{v_i,v_j} + \log N_{pos}) + \exp(p_{v_i,v_j} + \log N_{neg})}, \tag{12}$$

where p_{v_i,v_j} is the predicted consistency score for the pair (v_i, v_j) according to Eq. (8), and $\mathbb{I}(\cdot)$ is the indicator function. This loss effectively prevents the prediction bias and enables the discriminator to more accurately distinguish semantically consistent pairs.

3.3.2 Fine-tuning process

After the pre-training process, the initially calibrated graph encoder could produce relatively high-quality representations, while the relationship-consistency discriminator possesses a certain ability to detect semantic changes among sample pairs. It is proper to further enhance both components and drive them towards mutual reinforcement. Considering this, we adopt an alternating training strategy between the GNN encoder and the discriminator.

Encoder fine-tuning with calibrated supervision. In each iteration, we first obtain two augmented graph views U and V of the input graph with graph augmentations, then follow the procedure in Section 3.2 to yield the fusion representation matrices $\boldsymbol{Z}_U$ and $\boldsymbol{Z}_V$ for the two augmented views. These matrices are used for constructing the intra-view pairs $(\boldsymbol{Z}_U, \boldsymbol{Z}_U)$, $(\boldsymbol{Z}_V, \boldsymbol{Z}_V)$ and inter-view pair $(\boldsymbol{Z}_U, \boldsymbol{Z}_V)$ as the input of the discriminator. The discriminator then estimates the consistency score of each sample pair among these fusion representation pairs to further calibrate the encoder through the calibrated contrastive loss:

$$\ell_{cali}(u_i) = \\ -\log \frac{\sum_j \tilde{l}_{u_i,v_j} \cdot \mathcal{S}_{part}(\boldsymbol{h}_{u_i}, \boldsymbol{h}_{v_j}) + \sum_{j \neq i} \tilde{l}_{u_i,u_j} \cdot \mathcal{S}_{part}(\boldsymbol{h}_{u_i}, \boldsymbol{h}_{u_j})}{\sum_i \tilde{l}_{u_i,v_i} \cdot \mathcal{S}_{part}(\boldsymbol{h}_{u_i}, \boldsymbol{h}_{v_i}) + \sum_j \tilde{l}'_{u_i,v_j} \cdot \mathcal{S}_{part}(\boldsymbol{h}_{u_i}, \boldsymbol{h}_{v_j}) + \sum_{j \neq i} \tilde{l}'_{u_i,u_j} \cdot \mathcal{S}_{part}(\boldsymbol{h}_{u_i}, \boldsymbol{h}_{u_j})}, \tag{13}$$

where $\tilde{l}_{u_i,v_j} = \mathbb{I}(p_{u_i,v_j} \geq \eta)$ represents the consistency label between u_i and v_j by inputting the corresponding fusion representation into the discriminator, and $\tilde{l}'_{u_i,v_j} = 1 - \tilde{l}_{u_i,v_j}$. Additionally, we only add the positive sample pairs with the highest confidence in the denominator to reduce computation cost, where an adopted sample pair is judged as positive by the discriminator and includes corresponding samples between the augmentation views. This calibrated contrastive loss promotes alignment between consistent pairs while suppressing misleading or semantically flipped pairs that arise from graph augmentations. Similarly, we have the overall loss for fine-tuning GNN as

$$\mathcal{L}_{cali} = \frac{1}{2N} \sum_{i=1}^{N} \left[\ell_{cali}(u_i) + \ell_{cali}(v_i) \right]. \tag{14}$$

Table 1: Empirical results of self-supervised representation learning in node classification. The best results are highlighted in **bold**, and the second-best results are highlighted with underline.

Dataset	Cora	Citeseer	Pubmed	DBLP	Photo	Computers
AFGRL	83.34 ± 0.87	71.49 ± 0.78	85.21 ± 0.22	83.08 ± 0.14	93.22 ± 0.28	89.88 ± 0.33
SUGRL	85.37 ± 0.55	73.49 ± 0.66	86.68 ± 0.21	83.03 ± 0.23	93.20 ± 0.40	88.90 ± 0.20
NCLA	85.32 ± 0.44	73.24 ± 0.55	85.47 ± 0.40	83.97 ± 0.17	93.48 ± 0.22	89.14 ± 0.35
GREET	85.70 ± 0.46	73.26 ± 0.60	86.95 ± 0.31	83.81 ± 0.13	92.85 ± 0.31	87.94 ± 0.35
HomoGCL	85.40 ± 0.46	72.34 ± 0.40	86.31 ± 0.18	84.39 ± 0.16	93.25 ± 0.26	90.09 ± 0.32
S2GAE	85.46 ± 0.28	73.37 ± 0.47	86.46 ± 0.09	84.08 ± 0.00	93.50 ± 0.16	89.99 ± 0.14
iGCL	84.31 ± 0.43	72.85 ± 0.85	86.17 ± 0.25	83.74 ± 0.23	93.10 ± 0.26	90.06 ± 0.41
PiGCL	84.63 ± 0.78	73.51 ± 0.64	86.30 ± 0.20	84.30 ± 0.28	93.14 ± 0.30	89.25 ± 0.27
Bandana	85.48 ± 0.84	73.04 ± 0.75	86.35 ± 0.25	83.93 ± 0.02	93.44 ± 0.11	89.62 ± 0.09
SGRL	85.36 ± 0.23	73.20 ± 0.22	86.17 ± 0.01	84.12 ± 0.01	**93.83 ± 0.04**	90.02 ± 0.02
CaliGCL	**85.87 ± 0.62**	**74.13 ± 0.54**	**87.16 ± 0.19**	**85.32 ± 0.13**	93.72 ± 0.24	**90.79 ± 0.28**

Discriminator enhancement with updated representations. Discriminator fine-tuning is similar to the pre-training, but differs in the sample selection strategy. Since the semantic shift bias of the encoder is alleviated by the discriminator, the produced representations of the encoder are more reliable. Considering this, we apply the k-NN algorithm in the representation space to pick out the positives and negatives rather than the original feature space. These pairs are used to update the discriminator with Eq. (12), allowing it to more accurately model semantic consistency based on progressively refined representations.

4 Experiments

In this section, we evaluate our proposed model across multiple widely used graph datasets, including citation networks (**Cora**, **Citeseer**, **Pubmed**, and **DBLP**), co-purchase networks (**Amazon Photo**, and **Amazon Computers**), social networks (**COLLAB**, **REDDIT-BINARY**, **REDDIT-MULTI-5K**, **IMDB-BINARY**), and biochemical networks (**NCI1**, **PROTEINS**, **DD**, and **MUTAG**). The detailed dataset information and hyperparameter settings for these datasets are provided in the Appendix B. In the comparative experiments, the node classification and graph classification are employed to evaluate the model expressiveness. For fair comparison, we compare our model with recent state-of-the-art self-supervised graph models for each task. All the experiments are implemented in Pytorch and conducted on a server with RTX 3090 (24 GB).

4.1 Node classification

In node classification, we compare our model against both contrastive and generative graph representation learning methods, including **AFGRL** [11], **SUGRL** [32], **NCLA** [26], **GREET** [33], **HomoGCL** [27], **S2GAE** [34], **iGCL** [35], **PiGCL** [36], **Bandana** [37], and **SGRL** [38]. In our evaluation pipeline, the raw graph is first encoded to produce node representations, which are then employed for training a linear classifier. Due to the weakness of the linear classifier, the performance mainly depends on the representation quality. In our experiment setting, we split 10% representations for training the classifier, 10% for validation, and the remainder for testing. We report the mean F1 with standard deviation to evaluate the performance, and repeat experiments 10 times to provide reliable outcomes in Table 1.

The comparison results reveal that our model is competitive or even surpasses other baselines, which validates the model effectiveness. Additionally, we have the following observations:
(1) GCL models that solely rely on cross-view positives, such as GCA and PiGCL, show inferior performance to other models incorporating the extra neighbor positives, e.g., NCLA, GREET, and HomoGCL. It suggests the significance of calibrating the contrastive supervision.
(2) Generative models like S2GAE and Bandana, which focus on reconstructing graph topology, achieve performance on par with powerful contrastive methods. This supports the homophily principle and further explains why those GCL models focusing on local consistency perform well.
(3) The proposed CaliGCL effectively calibrates the similarity estimation bias and semantic shift bias in GCL, showing best performance on nearly all the datasets. It signifies that CaliGCL has sufficient

Table 2: Comparisons with different graph models in graph classification. The best results are highlighted in **bold**, and the second-best results are highlighted with underline.

Datasets	Biochemical Molecules			Social Networks			
	NCI1	DD	MUTAG	COLLAB	RDT-B	RDT-M5K	IMDB-B
InfoGCL	76.2 ± 1.1	72.9 ± 1.8	89.0 ± 1.1	70.7 ± 1.1	82.5 ± 1.4	53.5 ± 1.0	73.0 ± 0.9
GraphCL	77.9 ± 0.4	78.6 ± 0.4	86.8 ± 1.4	71.4 ± 1.2	89.5 ± 0.8	56.0 ± 0.3	71.1 ± 0.4
JOAO	78.1 ± 0.5	77.3 ± 0.5	87.4 ± 1.0	69.5 ± 0.4	85.3 ± 1.4	55.7 ± 0.6	70.2 ± 3.1
JOAOv2	78.4 ± 0.5	77.4 ± 1.2	87.7 ± 0.8	69.3 ± 0.3	86.4 ± 1.5	56.0 ± 0.2	70.8 ± 0.3
AD-GCL	69.7 ± 0.5	74.5 ± 0.5	88.6 ± 1.3	73.3 ± 0.6	85.5 ± 0.8	53.0 ± 0.8	71.6 ± 1.0
SimGRACE	79.1 ± 0.4	77.4 ± 1.1	89.0 ± 1.3	71.7 ± 0.8	89.5 ± 0.9	55.9 ± 0.3	71.3 ± 0.8
SPAN	71.4 ± 0.5	75.8 ± 0.5	89.1 ± 0.8	75.0 ± 0.5	83.6 ± 0.6	54.1 ± 0.5	73.7 ± 0.7
GPA	80.4 ± 0.4	79.9 ± 0.4	89.7 ± 0.8	76.2 ± 0.1	89.3 ± 0.4	53.7 ± 0.2	74.6 ± 0.4
DRGCL	79.7 ± 0.4	78.4 ± 0.7	89.5 ± 0.6	70.6 ± 0.8	**90.8 ± 0.3**	56.3 ± 0.2	72.0 ± 0.5
CaliGCL	**80.8 ± 2.0**	**80.4 ± 2.5**	**90.4 ± 5.8**	**77.2 ± 1.7**	90.3 ± 2.7	**56.5 ± 1.5**	**76.9 ± 5.0**

competence to distinguish its positives and negatives, benefiting the downstream classification task. (4) While CaliGCL performs well on smaller datasets such as Cora and Citeseer, it exhibits even stronger improvements on larger datasets like DBLP and Computers. This highlights its ability to uncover and utilize latent positives that are often neglected by the conventional contrastive loss.

The superior performance of CaliGCL stems from its ability to calibrate both the similarity estimation bias and semantic shift bias in GCL, which allows CaliGCL to identify latent positive pairs and remove spurious negatives, ultimately leading to more discriminative representations.

4.2 Graph classification

In this experiment, we evaluate the performance of CaliGCL on the graph classification task under an unsupervised learning setting, following standard protocols introduced in [39] and [40]. Different from the node classification, the positives based on the k-NN algorithm are difficult to obtain since graph datasets may lack feature information. Thus, the discriminator is not pre-trained and ignores the structure information.

For the experiment setting, we first train a GIN encoder and then train an SVM classifier to classify the produced graph representations via 10-fold cross-validation. Our proposed model is compared with recent self-supervised graph models, including **InfoGCL** [41], **GraphCL** [39], **JOAO** and **JOAOv2** [42], **AD-GCL** [43], **SimGRACE** [43], **SPAN** [44], **GPA** [40], and **DRGCL** [45]. According to the results in Table 2, we have the following observations:
(1) When compared with the augmentation-free model SimGRACE, CaliGCL preserves the augmentations to realize sample diversity, which is crucial for effective GCL learning. Moreover, CaliGCL mitigates the adverse effects of the augmentations by calibrating the biases inherent in GCL.
(2) CaliGCL still outperforms models that employ learnable augmentations, such as GPA. This superiority is attributed to the competence of debiasing semantic shift, which is also neglected by models that only optimize augmentation strength or combination strategies, without considering their potential to distort semantic consistency between sample pairs.

Overall, the graph classification results confirm that CaliGCL could also boost the graph-level task by adapting a contrastive learning framework to work on graph-level representations. This highlights the flexibility and robustness of the proposed framework in self-supervised learning settings.

4.3 Hyperparameter analysis

we conduct a sensitivity analysis on the temperature coefficient τ and the partition size m, and report the mean F1 as the model performance in Figure 3. Figure 3(a) and (b) show that the performance changes over different values of τ, indicating that the temperature coefficient is critical for distinguishing the positives and negatives. Figure 3(c) and (d) demonstrate that partitions with an appropriate number of feature elements m can improve the model performance. This supports the effectiveness of partitioning the representation vectors to calibrate fine-grained semantic structures. However, more partitions may introduce variance and degrade the performance.

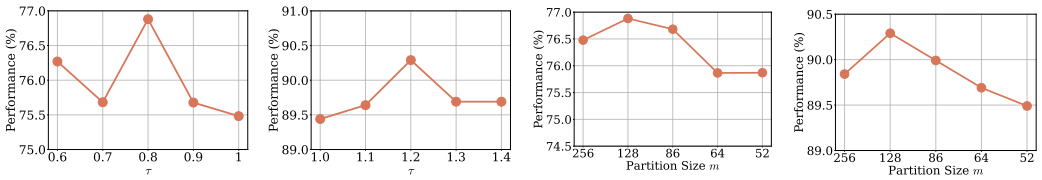

(a) IMDB-B (b) RDT-B (c) IMDB-B (d) RDT-B

Figure 3: Hyperparameter analysis on the temperature coefficient τ and the partition size m.

5 Conclusion

In this paper, we identify two biases in GCL: similarity estimation bias caused by conflicts between positively- and negatively-synergistic features, and semantic shift bias introduced by random augmentations. To mitigate the issues, we propose CaliGCL to enhance the influence of positively-synergistic features while suppressing negative ones, and correct semantic inconsistencies in contrastive pairs. However, the exponential partitioned similarity measure is not adaptive, and it could be further enhanced by automatically distinguishing the positively- and negatively-synergestic features.

Acknowledgments and Disclosure of Funding

This work was supported by the National Natural Science Foundation of China (No. 62306020), the Young Elite Scientist Sponsorship Program by BAST (No. BYESS2024199), Beijing Natural Science Foundation (No. L244009), the National Key Research and Development Program of China (No. 2023YFB3107100), and partially supported by the Central Guidance for Local Scientific and Technological Development Fund (No.2024ZY0124). The first author is funded by the China Scholarship Council (CSC) from the Ministry of Education, China.

References

[1] Jiaming Zhuo, Yintong Lu, Hui Ning, Kun Fu, Dongxiao He, Chuan Wang, Yuanfang Guo, Zhen Wang, Xiaochun Cao, Liang Yang, et al. Unified graph augmentations for generalized contrastive learning on graphs. *Advances in Neural Information Processing Systems*, pages 37473–37503, 2024.

[2] Yanqiao Zhu, Yichen Xu, Feng Yu, Qiang Liu, Shu Wu, and Liang Wang. Deep graph contrastive representation learning. In *International Conference on Machine Learning*, pages 1–17, 2020.

[3] Yuena Lin, Haichun Cai, Jun-Yi Hang, Haobo Wang, Zhen Yang, and Gengyu Lyu. Mitigating local cohesion and global sparseness in graph contrastive learning with fuzzy boundaries. In *International Conference on Machine Learning*, pages 1–17, 2025.

[4] Jie Xu, Huayi Tang, Yazhou Ren, Liang Peng, Xiaofeng Zhu, and Lifang He. Multi-level feature learning for contrastive multi-view clustering. In *Proceedings of the IEEE/CVF Conference on Computer Vision and Pattern Recognition*, pages 16051–16060, 2022.

[5] Zhuo Li, Yuena Lin, Yipeng Wang, Wenmao Liu, Mingliang Yu, Zhen Yang, and Gengyu Lyu. Critical node-aware augmentation for hypergraph contrastive learning. pages 5671–5679, 2025.

[6] Jie Xu, Shuo Chen, Yazhou Ren, Xiaoshuang Shi, Hengtao Shen, Gang Niu, and Xiaofeng Zhu. Self-weighted contrastive learning among multiple views for mitigating representation degeneration. *Advances in Neural Information Processing Systems*, pages 1–13, 2024.

[7] Jing Wang, Songhe Feng, Gengyu Lyu, and Zhibin Gu. Triple-granularity contrastive learning for deep multi-view subspace clustering. In *Proceedings of the ACM international conference on multimedia*, pages 2994–3002, 2023.

[8] Yuena Lin, Gengyu Lyu, Haichun Cai, Deng-Bao Wang, Haobo Wang, and Zhen Yang. Simplified graph contrastive learning model without augmentation. *IEEE Transactions on Knowledge and Data Engineering*, 37(10):6159–6172, 2025.

[9] Sylvestre-Alvise Rebuffi, Sven Gowal, Dan Andrei Calian, Florian Stimberg, Olivia Wiles, and Timothy A Mann. Data augmentation can improve robustness. *Advances in Neural Information Processing Systems*, 34:29935–29948, 2021.

[10] Yonghua Zhu, Lei Feng, Zhenyun Deng, Yang Chen, Robert Amor, and Michael Witbrock. Robust node classification on graph data with graph and label noise. In *Proceedings of the AAAI Conference on Artificial Intelligence*, pages 17220–17227, 2024.

[11] Namkyeong Lee, Junseok Lee, and Chanyoung Park. Augmentation-free self-supervised learning on graphs. In *Proceedings of the AAAI Conference on Artificial Intelligence*, pages 7372–7380, 2022.

[12] Xihong Yang, Cheng Tan, Yue Liu, Ke Liang, Siwei Wang, Sihang Zhou, Jun Xia, Stan Z Li, Xinwang Liu, and En Zhu. Convert: Contrastive graph clustering with reliable augmentation. In *Proceedings of the 31st ACM International Conference on Multimedia*, pages 319–327, 2023.

[13] Hongliang Chi and Yao Ma. Enhancing contrastive learning on graphs with node similarity. In *Proceedings of the ACM SIGKDD Conference on Knowledge Discovery and Data Mining*, pages 456–465, 2024.

[14] Zhiqiang Kou, Jing Wang, Yuheng Jia, Biao Liu, and Xin Geng. Instance-dependent inaccurate label distribution learning. *IEEE Transactions on Neural Networks and Learning Systems*, 36(1):1425–1437, 2025.

[15] Zhiqiang Kou, Jing Wang, Yuheng Jia, and Xin Geng. Progressive label enhancement. *Pattern Recognition*, 160:111172, 2025.

[16] Qianqian Wang, Zhengming Ding, Zhiqiang Tao, Quanxue Gao, and Yun Fu. Generative partial multi-view clustering with adaptive fusion and cycle consistency. *IEEE Transactions on Image Processing*, 30:1771–1783, 2021.

[17] Qianqian Wang, Zhiqiang Tao, Wei Xia, Quanxue Gao, Xiaochun Cao, and Licheng Jiao. Adversarial multiview clustering networks with adaptive fusion. *IEEE Transactions on Neural Networks and Learning Systems*, 34(10):7635–7647, 2023.

[18] Chuan Shi, Houye Ji, Zhiyuan Lu, Ye Tang, Pan Li, and Cheng Yang. Distance information improves heterogeneous graph neural networks. *IEEE Transactions on Knowledge and Data Engineering*, 36(3):1030–1043, 2024.

[19] Xiang Deng, Songhe Feng, Gengyu Lyu, Tao Wang, and Congyan Lang. Beyond word embeddings: Heterogeneous prior knowledge driven multi-label image classification. *IEEE Transactions on Multimedia*, 25:4013–4025, 2022.

[20] Gengyu Lyu, Yanan Wu, and Songhe Feng. Deep graph matching for partial label learning. In *International Joint Conference on Artificial Intelligence*, pages 3306–3312, 2022.

[21] Keyulu Xu, Weihua Hu, Jure Leskovec, and Stefanie Jegelka. How powerful are graph neural networks? In *International Conference on Learning Representations*, pages 1–17, 2019.

[22] Aaron van den Oord, Yazhe Li, and Oriol Vinyals. Representation learning with contrastive predictive coding. *arXiv preprint arXiv:1807.03748*, pages 1–13, 2018.

[23] Qianqian Wang, Zhiqiang Tao, Quanxue Gao, and Licheng Jiao. Multi-view subspace clustering via structured multi-pathway network. *IEEE Transactions on Neural Networks and Learning Systems*, 35(5):7244–7250, 2024.

[24] Yanqiao Zhu, Yichen Xu, Feng Yu, Qiang Liu, Shu Wu, and Liang Wang. Graph contrastive learning with adaptive augmentation. In *Proceedings of the Web Conference*, pages 2069–2080, 2021.

[25] Yifei Zhang, Hao Zhu, Zixing Song, Piotr Koniusz, and Irwin King. Costa: covariance-preserving feature augmentation for graph contrastive learning. In *Proceedings of the 28th ACM SIGKDD Conference on Knowledge Discovery and Data Mining*, pages 2524–2534, 2022.

[26] Xiao Shen, Dewang Sun, Shirui Pan, Xi Zhou, and Laurence T Yang. Neighbor contrastive learning on learnable graph augmentation. In *Proceedings of the AAAI Conference on Artificial Intelligence*, pages 9782–9791, 2023.

[27] Wen-Zhi Li, Chang-Dong Wang, Hui Xiong, and Jian-Huang Lai. Homogcl: Rethinking homophily in graph contrastive learning. In *Proceedings of the 29th ACM SIGKDD Conference on Knowledge Discovery and Data Mining*, pages 1341–1352, 2023.

[28] Jinsong Chen, Kaiyuan Gao, Gaichao Li, and Kun He. Nagphormer: A tokenized graph transformer for node classification in large graphs. In *International Conference on Learning Representations*, pages 1–18, 2023.

[29] Thomas N Kipf and Max Welling. Semi-supervised classification with graph convolutional networks. In *International Conference on Learning Representations*, pages 1–14, 2017.

[30] Jiawei Ren, Cunjun Yu, Xiao Ma, Haiyu Zhao, Shuai Yi, and Hongsheng Li. Balanced meta-softmax for long-tailed visual recognition. *Advances in Neural Information Processing Systems*, pages 4175–4186, 2020.

[31] Mengting Zhou and Zhiguo Gong. Neighbor distribution learning for minority class augmentation. *IEEE Transactions on Knowledge and Data Engineering*, 33(12):8901–8913, 2024.

[32] Yujie Mo, Liang Peng, Jie Xu, Xiaoshuang Shi, and Xiaofeng Zhu. Simple unsupervised graph representation learning. In *Proceedings of the AAAI Conference on Artificial Intelligence*, pages 7797–7805, 2022.

[33] Yixin Liu, Yizhen Zheng, Daokun Zhang, Vincent CS Lee, and Shirui Pan. Beyond smoothing: Unsupervised graph representation learning with edge heterophily discriminating. In *Proceedings of the AAAI Conference on Artificial Intelligence*, pages 4516–4524, 2023.

[34] Qiaoyu Tan, Ninghao Liu, Xiao Huang, Soo-Hyun Choi, Li Li, Rui Chen, and Xia Hu. S2gae: Self-supervised graph autoencoders are generalizable learners with graph masking. In *Proceedings of the sixteenth ACM International Conference on Web Search and Data Mining*, pages 787–795, 2023.

[35] Haifeng Li, Jun Cao, Jiawei Zhu, Qinyao Luo, Silu He, and Xuying Wang. Augmentation-free graph contrastive learning of invariant-discriminative representations. *IEEE Transactions on Neural Networks and Learning Systems*, 35(8):11157–11167, 2024.

[36] Dongxiao He, Jitao Zhao, Cuiying Huo, Yongqi Huang, Yuxiao Huang, and Zhiyong Feng. A new mechanism for eliminating implicit conflict in graph contrastive learning. In *Proceedings of the AAAI Conference on Artificial Intelligence*, pages 12340–12348, 2024.

[37] Ziwen Zhao, Yuhua Li, Yixiong Zou, Jiliang Tang, and Ruixuan Li. Masked graph autoencoder with non-discrete bandwidths. In *Proceedings of the ACM Web Conference*, pages 377–388, 2024.

[38] Dongxiao He, Lianze Shan, Jitao Zhao, Hengrui Zhang, Zhen Wang, and Weixiong Zhang. Exploitation of a latent mechanism in graph contrastive learning: Representation scattering. In *Advances in Neural Information Processing Systems*, pages 1–26, 2024.

[39] Yuning You, Tianlong Chen, Yongduo Sui, Ting Chen, Zhangyang Wang, and Yang Shen. Graph contrastive learning with augmentations. *Advances in Neural Information Processing Systems*, pages 5812–5823, 2020.

[40] Xin Zhang, Qiaoyu Tan, Xiao Huang, and Bo Li. Graph contrastive learning with personalized augmentation. *IEEE Transactions on Knowledge and Data Engineering*, 36(11):6305–6316, 2024.

[41] Fan-Yun Sun, Jordan Hoffman, Vikas Verma, and Jian Tang. Infograph: Unsupervised and semi-supervised graph-level representation learning via mutual information maximization. In *International Conference on Learning Representations*, pages 1–16, 2020.

[42] Yuning You, Tianlong Chen, Yang Shen, and Zhangyang Wang. Graph contrastive learning automated. In *International Conference on Machine Learning*, pages 12121–12132. PMLR, 2021.

[43] Susheel Suresh, Pan Li, Cong Hao, and Jennifer Neville. Adversarial graph augmentation to improve graph contrastive learning. *Advances in Neural Information Processing Systems*, pages 15920–15933, 2021.

[44] Lu Lin, Jinghui Chen, and Hongning Wang. Spectral augmentation for self-supervised learning on graphs. In *International Conference on Learning Representations*, pages 1–27, 2023.

[45] Qirui Ji, Jiangmeng Li, Jie Hu, Rui Wang, Changwen Zheng, and Fanjiang Xu. Rethinking dimensional rationale in graph contrastive learning from causal perspective. In *Proceedings of the AAAI Conference on Artificial Intelligence*, pages 12810–12820, 2024.

A Theorem proofs

A.1 The proof of Theorem 1

Proof. Let $\boldsymbol{h}_{u,i}$ and $\boldsymbol{h}_{v,i}$ be the i-th elements of $\boldsymbol{h}_u$ and $\boldsymbol{h}_v$, respectively. Since $\boldsymbol{h}_{u,i}$ and $\boldsymbol{h}_{v,i}$ are i.i.d., then the expectation of $\boldsymbol{h}_{u,i}\boldsymbol{h}_{v,i}$ is

$$\mathbb{E}[\boldsymbol{h}_{u,i}\boldsymbol{h}_{v,i}] = \mathbb{E}[\boldsymbol{h}_{u,i}]\mathbb{E}[\boldsymbol{h}_{v,i}] = \mu^2. \tag{15}$$

Based on this, the expectation of the inner product over m ($m \leq d$) features is

$$\sum_{i=1}^{m} \mathbb{E}[\boldsymbol{h}_{u,i}\boldsymbol{h}_{v,i}] = m\mu^2. \tag{16}$$

For $\boldsymbol{h}_{u,i}, \boldsymbol{h}_{u,i} \sim \mathcal{N}(\mu, \sigma^2)$, we have

$$\mathbb{E}[\boldsymbol{h}_{u,i}^2] = \text{Var}(\boldsymbol{h}_{u,i}) + (\mathbb{E}[\boldsymbol{h}_{u,i}])^2 = \sigma^2 + \mu^2, \tag{17}$$

Similarly, we have $\mathbb{E}[\boldsymbol{h}_{v,i}^2] = \sigma^2 + \mu^2$. Thus, the expectation of $\boldsymbol{h}_{u,i}^2\boldsymbol{h}_{v,i}^2$ is

$$\mathbb{E}[\boldsymbol{h}_{u,i}^2\boldsymbol{h}_{v,i}^2] = (\sigma^2 + \mu^2)^2. \tag{18}$$

Then the variance of $\boldsymbol{h}_{u,i}\boldsymbol{h}_{v,i}$ is calculated as

$$\text{Var}(\boldsymbol{h}_{u,i}\boldsymbol{h}_{v,i}) = \mathbb{E}[\boldsymbol{h}_{u,i}^2\boldsymbol{h}_{v,i}^2] - (\mathbb{E}[\boldsymbol{h}_{u,i}\boldsymbol{h}_{v,i}])^2 = (\sigma^2 + \mu^2)^2 - \mu^4 = \mu^4 + 2\mu^2\sigma^2. \tag{19}$$

Since $\boldsymbol{h}_{u,i}$ and $\boldsymbol{h}_{v,i}$ are independent, we have

$$\text{Var}\left(\sum_{i=1}^{m} \boldsymbol{h}_{u,i}\boldsymbol{h}_{v,i}\right) = m(\mu^4 + 2\mu^2\sigma^2). \tag{20}$$

Therefore, by the Central Limit Theorem, we have $\sum_{i=1}^{m} \boldsymbol{h}_{u,i}\boldsymbol{h}_{v,i} \sim \mathcal{N}(m\mu^2, m(\mu^2 + 2\sigma^2)^2)$. Finally, the probability that $\sum_{i=1}^{m} \boldsymbol{h}_{u,i}\boldsymbol{h}_{v,i} < 0$ is

$$\mathbb{P}\left(\sum_{i=1}^{m} \boldsymbol{h}_{u,i}\boldsymbol{h}_{v,i} < 0\right) = \Phi\left(\frac{-m\mu^2}{\sqrt{m(\mu^2 + 2\sigma^2)^2}}\right). \tag{21}$$

A.2 The proof of Theorem 2

Proof. We consider the temperature coefficient $\tau = 1$ for both the exponential partitioned similarity and the exponential inner product similarity. For a pair $(\boldsymbol{h}_u, \boldsymbol{h}_v)$, we have the standard exponential inner product similarity defined as:

$$\mathcal{S}(\boldsymbol{h}_u, \boldsymbol{h}_v) = \exp(\boldsymbol{h}_u^\top \boldsymbol{h}_v) = \exp\left(\sum_{k=1}^{K} \boldsymbol{h}_u^{(k)\top} \boldsymbol{h}_v^{(k)}\right),$$

where $\mathcal{S}(\cdot)$ denotes the exponential inner product similarity, and $\boldsymbol{h}_u^{(k)}$, $\boldsymbol{h}_v^{(k)}$ are the k-th partitions of representations $\boldsymbol{h}_u$ and $\boldsymbol{h}_v$, respectively. The exponential partitioned similarity measure is defined as

$$\mathcal{S}_{part}(\boldsymbol{h}_u, \boldsymbol{h}_v) = \frac{1}{K}\sum_{k=1}^{K} \exp\left(\boldsymbol{h}_u^{(k)\top} \boldsymbol{h}_v^{(k)}\right). \tag{22}$$

By Jensen's inequality and the convexity of the exponential function, for all $\mathcal{S}_1, \mathcal{S}_2, \ldots, \mathcal{S}_K \in \mathbb{R}$ (each representing the inner product of a partition), we have

$$\exp\left(\frac{1}{K}\sum_{k=1}^{K} \mathcal{S}_k\right) \leq \frac{1}{K}\sum_{k=1}^{K} \exp(\mathcal{S}_k), \tag{23}$$

which leads to

$$\exp\left(\sum_{k=1}^{K} \mathcal{S}_k\right) \leq \frac{1}{K}\sum_{k=1}^{K} \exp(K\mathcal{S}_k), \tag{24}$$

This inequality corresponds to

$$\mathcal{S}(\boldsymbol{h}_u, \boldsymbol{h}_v) \leq \mathcal{S}_{part}(\boldsymbol{h}_u, \boldsymbol{h}_v). \tag{25}$$

A.3 The proof of Theorem 3

To prove the theorem, we first provide the following **Lemma 4** as

Lemma 4 *Let $\boldsymbol{h}$ and $\boldsymbol{h}^+$ be positive sample pairs drawn from a joint distribution $p(\boldsymbol{h}, \boldsymbol{h}^+)$, and let $\mathcal{S}_{part}(\boldsymbol{h}, \boldsymbol{h}') = \frac{1}{K}\sum_{k=1}^{K} \exp\left(\frac{K}{\tau} \cdot \boldsymbol{h}^{(k)\top}\boldsymbol{h}'^{(k)}\right)$ denote the exponential partitioned similarity between two representations. Define the partitioned contrastive loss as:*

$$\mathcal{L}_{part} = -\mathbb{E}_{\boldsymbol{h},\boldsymbol{h}^+}\left[\log \frac{\mathcal{S}_{part}(\boldsymbol{h}, \boldsymbol{h}^+)}{\sum_{\boldsymbol{h}'} \mathcal{S}_{part}(\boldsymbol{h}, \boldsymbol{h}')}\right],$$

Then, the following lower bound on mutual information holds:

$$I(\boldsymbol{h}; \boldsymbol{h}^+) \geq \log N - \mathcal{L}_{part}.$$

where N is the number of samples.

Proof. This result follows from the lower bound of mutual information derived in [22], which shows that any InfoNCE-style loss of the form:

$$\mathcal{L}_{NCE} = -\mathbb{E}_{\boldsymbol{h},\boldsymbol{h}^+}\left[\log \frac{p(\boldsymbol{h}^+|\boldsymbol{h})}{\sum_{\boldsymbol{h}'} p(\boldsymbol{h}'|\boldsymbol{h})}\right] \tag{26}$$

satisfies the lower bound $I(\boldsymbol{h}; \boldsymbol{h}^+) \geq \log N - \mathcal{L}_{NCE}$ for any positive scoring function $p(\boldsymbol{h}^+|\boldsymbol{h})$ approximating the true density ratio. In our case, we define $p(\boldsymbol{h}^+|\boldsymbol{h}) \propto \mathcal{S}_{part}(\boldsymbol{h}, \boldsymbol{h}^+)$, which is strictly positive and normalized over the dataset set via softmax. Therefore, the loss $\mathcal{L}_{part}$ conforms to the InfoNCE formulation and inherits the same mutual information lower bound.

Based on **Lemma 4**, the proof of **Theorem 3** is transformed to prove that $\mathcal{L}_{part}$ is the lower bound of $\mathcal{L}_{NCE}$. Therefore, we provide the following proof.

For a positive pair, its inner product similarity $\mathcal{S}^+$ obeys the following distribution:

$$\mathcal{S}^+ = \sum_{k=1}^{K} \mathcal{S}^{(k)+} \sim \mathcal{N}(K\mu_1, K\sigma_1^2). \tag{27}$$

Similarly, the distribution for the inner product similarity of a negative pair $\mathcal{S}^-$ is

$$\mathcal{S}^- = \sum_{k=1}^{K} \mathcal{S}^{(k)-} \sim \mathcal{N}(K\mu_2, K\sigma_2^2). \tag{28}$$

Then the original contrastive loss for a sample pair is defined as:

$$\mathcal{L}_{ct} = -\log \frac{\exp(\mathcal{S}^+)}{\exp(\mathcal{S}^+) + \sum_j \exp(\mathcal{S}_j^-)}, \tag{29}$$

where $\mathcal{S}^+$ is the inner product similarity between a positive pair, and $\mathcal{S}_j^-$ represents the inner product similarity between any other negative pair. Similarly, the partition contrastive loss is given by

$$\begin{aligned}\mathcal{L}_{ct-part} &= -\log \frac{\frac{1}{K}\sum_k \exp(K\mathcal{S}_{part}^{(k)+})}{\frac{1}{K}\sum_k \exp(K\mathcal{S}_{part}^{(k)+}) + \frac{1}{K}\sum_j \sum_k \exp(K\mathcal{S}_{part,j}^{(k)-})} \\ &= -\log \frac{\sum_k \exp(K\mathcal{S}_{part}^{(k)+})}{\sum_k \exp(K\mathcal{S}_{part}^{(k)+}) + \sum_j \sum_k \exp(K\mathcal{S}_{part,j}^{(k)-})}\end{aligned}, \tag{30}$$

where $S_{part}^{(k)+}$ is the inner product similarity of the k-th partition between a positive pair, and $S_{part,j}^{(k)-}$ represents the inner product similarity of the k-th partition between a negative pair.

Let

$$\begin{cases} A = \exp(\mathcal{S}^+) \\ \widetilde{A} = \sum_k \exp(K\mathcal{S}_{part}^{(k)+}) \\ B = \exp(\mathcal{S}^+) + \sum_j \mathcal{S}_j^- \\ \widetilde{B} = \sum_k \exp(K\mathcal{S}_{part}^{(k)+}) + \sum_j \sum_k \exp(K\mathcal{S}_{part,j}^{(k)-}) \end{cases}, \tag{31}$$

the comparison between the two losses is transformed to compare $\frac{\tilde{A}}{\tilde{B}}$ with $\frac{A}{B}$.

Let

$$\begin{cases} \alpha = \frac{\tilde{A}}{\tilde{B}} \\ \beta = \frac{A}{B} \\ P_1 = \mathbb{E}[\exp(\mathcal{S}^+)] \\ P_2 = \mathbb{E}[\exp(K \cdot \mathcal{S}^{(k)+})] \\ Q_1 = \mathbb{E}[\exp(\mathcal{S}^-)] \\ Q_2 = \mathbb{E}[\exp(K \cdot \mathcal{S}^{(k)-}_{part,j})] \end{cases}, \tag{32}$$

and we implement the expectations to approximate α and β:

Then we have

$$\alpha \approx \frac{P_2}{P_2 + (N-1)Q_2}, \quad \beta \approx \frac{P_1}{P_1 + (N-1)Q_1}. \tag{33}$$

Therefore, $\frac{\alpha}{\beta} \approx \frac{P_2[P_1+(N-1)Q_1]}{P_1[P_2+(N-1)Q_2]} = \frac{P_1P_2+(N-1)Q_1P_2}{P_1P_2+(N-1)Q_2P_1}$, it means that whether the ratio between α and β is greater depends on the comparison between Q_1P_2 and Q_2P_1.

According to the assumption that the inner product similarities of partitions follow the Gaussian distribution, the exponentials of the inner product similarities obey the log-normal distribution, and we have

$$\begin{cases} P_1 = \mathbb{E}[\exp(\mathcal{S}^+)] = \exp(K\mu_1 + \frac{K\sigma_1^2}{2}) \\ P_2 = \mathbb{E}[\exp(K \cdot \mathcal{S}^{(k)+})] = \exp(K\mu_1 + \frac{K^2\sigma_1^2}{2}) \\ Q_1 = \mathbb{E}[\exp(\mathcal{S}^-)] = \exp(K\mu_2 + \frac{K\sigma_2^2}{2}) \\ Q_2 = \mathbb{E}[\exp(K \cdot \mathcal{S}^{(k)-}_{part,j})] = \exp(K\mu_2 + \frac{K^2\sigma_2^2}{2}) \end{cases}. \tag{34}$$

We turn the comparison between Q_1P_2 and Q_2P_1 to the comparison between $\log\frac{P_1}{Q_1}$ and $\log\frac{P_2}{Q_2}$, then we have

$$\log\frac{P_1}{Q_1} - \log\frac{P_2}{Q_2} = \frac{K-K^2}{2}(\sigma_1^2 - \sigma_2^2). \tag{35}$$

Since $K \geq 1$, $K - K^2 \leq 0$. According to the assumption $\sigma_1^2 - \sigma_2^2 \geq 0$, we have

$$\log\frac{P_1}{Q_1} - \log\frac{P_2}{Q_2} \leq 0. \tag{36}$$

This means that the partition contrastive loss is the lower bound of the original contrastive loss, and the partition contrastive objective is an upper bound of mutual information than the original contrastive objective.

B Experiment

B.1 Datasets

We supplement the concrete descriptions of datasets in the following. Besides, the statistics of the datasets for learning node-level representations are shown in Table 3, and those for learning graph-level representations are shown in Table 4.

Cora, **CiteSeer**, **Pubmed**, and **DBLP** are four most widely used citation network datasets. In these datasets, each node represents a scientific paper, and the node attributes correspond to specific keywords extracted from the paper. An edge between two nodes indicates a citation relationship.

Amazon Photo and **Amazon Computers** are co-purchase networks, where nodes represent products and edges indicate that two products are frequently bought together. Node features are derived using a bag-of-words representation based on product descriptions.

NCI1 is a molecular graph dataset used for predicting chemical compounds' activity against cancer cells. **MUTAG** is another molecular dataset, commonly used for mutagenicity prediction. **DD** also contains chemical compounds and is employed in general graph classification tasks.

COLLAB is a social network dataset used for collaborative filtering. **REDDIT-BINARY** (RDT-B) consists of Reddit threads and is used for binary community classification. **IMDB-BINARY** (IMDB-B) is a dataset derived from movie collaboration networks, labeled for binary classification. **REDDIT-MULTI5K** (RDT-M5K) is a multi-class variant of the Reddit dataset, containing threads labeled into five categories.

Table 3: Statistics of different graph datasets for learning node-level representations.

Dataset	Cora	Citeseer	Pubmed	DBLP	Amazon Photo	Amazon Computers
Nodes	2,708	3,327	19,717	17,716	7,650	13,752
Edges	5,429	4,732	44,338	52,867	119,081	491,722
Features	1,433	3,703	500	1,639	745	767
Classes	7	6	3	4	8	10

Table 4: Statistics of different graph datasets for learning graph-level representations.

Data Type	Name	Graphs	Average Nodes	Average Edges	Classes
Biochemical Molecules	NCI1	4,110	29.87	32.30	2
	MUTAG	188	17.93	19.79	2
	DD	1,178	284.32	715.66	2
Social Networks	COLLAB	5,000	74.5	2457.78	3
	REDDIT-BINARY	2,000	429.6	497.75	2
	REDDIT-MULTI-5K	4,999	508.8	594.87	5
	IMDB-BINARY	1,000	19.8	96.53	2

B.2 Hyperparameter Setting

The hyperparameter settings for node and graph classification are listed in Table 5 and 6, respectively. For the hyperparameters used in the node-level datasets, Lr_Enc is the learning rate of the graph encoder in the pre-training phase, Epc_Init_Enc is the training epochs of the graph encoder in the pre-training phase, and Hid_dim is the hidden dimension of the graph encoder. Similarly, Lr_Dis, Epc_Init_Dis, Dis_dim, Dis_act are the learning rate, training epochs, hidden dimension, and activation function for the discriminator in the pre-training phase, respectively. Leaky represents LeakyReLU activation function. Itr_num is the number of iterations in the alternating training strategy, where the graph encoder is trained with Epc_FT_Enc epochs in each iteration and the discriminator is trained with Epc_FT_Dis epochs in each iteration. Proj_dim is the hidden dimension of the projector head, t is the dimension of the structure embedding, m is the number of feature elements in a partition, η is the threshold to distinguish the positive pairs and negative pairs for the discriminator, and τ is the temperature coefficient. p_{e1}, p_{f1}, p_{e2}, and p_{f2} are four hyperparameters for controlling the strength of graph augmentations. The hyperparameter settings in graph-level datasets are similar to he node-level datasets, but we abandon the structure embeddings since it is not appropriate to use node structure embeddings for constructing graph structure embeddings. Augmentation is the graph-level augmentation strategy adopted by the datasets, where 'dnodes' is to drop nodes, and 'random' includes node dropping, edge perturbation, attribute masking, and subgraph sampling. All the augmentations adopt the default ratio as [39].

B.3 Ablation study

We perform ablation studies to assess the contributions of the exponential partitioned similarity ("$\mathcal{S}_{part}$") and the semantics-consistency discriminator ("D") in the CaliGCL framework, and the results are reported in Figure 4. From the results, we could find that the exponential partitioned similarity and the discriminator could enhance the model performance. However, joint implementation of both methods can effectively alleviate the biases in GCL and further improve the model performance.

Table 5: Hyperparameter setting for node-level datasets.

Datasets	Cora	Citeseer	Pubmed	DBLP	Photo	Computers
Lr_Enc	1e-4	1e-3	3e-4	2e-4	5e-4	1e-3
Epc_Init_Enc	300	300	8000	1000	6000	9000
Hid_dim	[512,256]	[512,256]	[512,256]	[512,256]	[512,256]	[512,256]
Lr_Dis	4e-4	8e-4	8e-3	8e-3	8e-3	8e-4
Dis_dim	128	512	256	128	128	512
Dis_act	Leaky	Leaky	Leaky	Leaky	Leaky	Leaky
Epc_FT_Dis	10	10	10	5	5	20
Itr_num	25	15	30	5	1	15
Epc_FT_Enc	15	15	15	15	5	15
Epc_Init_Dis	25	10	25	150	40	25
Proj_dim	128	256	512	512	512	512
t	64	64	64	64	64	64
m	128	240	240	128	192	200
η	0.6	0.6	0.6	0.6	0.6	0.6
τ	0.8	0.9	0.23	1.2	0.1	0.1
p_{e1}	0.2	0.2	0.4	0.1	0.3	0.5
p_{f1}	0.3	0.3	0.0	0.4	0.1	0.2
p_{e2}	0.4	0.4	0.1	0.1	0.5	0.5
p_{f2}	0.4	0.5	0.2	0.0	0.1	0.1

Table 6: Hyperparameter setting for graph-level datasets.

Datasets	MUTAG	IMDB-B	COLLAB	RDT-B	DD	NCI1	RDT-M5K
Lr_Enc	2e-3	2e-3	1e-3	3e-3	4e-3	3e-3	1e-3
Epc_Init_Enc	40	40	270	80	90	270	270
Hid_dim	[128,128]	[128,128]	[256,128]	[128,128]	[256,256]	[128,128]	[128,128]
Epc_FT_Enc	15	15	15	15	15	15	15
Lr_Dis	8e-3	8e-3	8e-3	8e-3	8e-3	8e-3	8e-3
Dis_dim	128	128	128	128	64	64	128
Dis_act	Leaky	Leaky	Leaky	Leaky	Leaky	Leaky	Leaky
Epc_FT_Dis	5	5	5	5	10	10	5
Itr_num	5	5	5	5	5	5	5
Proj_dim	128	128	256	128	256	256	256
Augmentation	dnodes	random	dnodes	dnodes	dnodes	dnodes	dnodes
m	128	128	128	128	128	256	128
η	0.6	0.6	0.6	0.6	0.6	0.6	0.6
τ	0.7	0.8	0.05	1.2	0.1	0.05	0.04

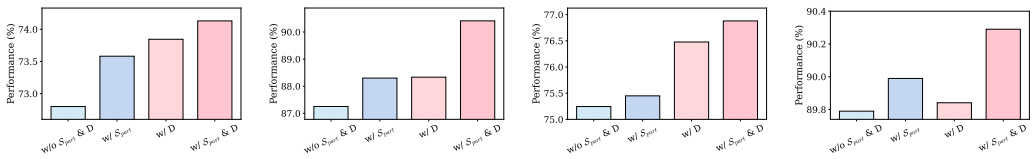

(a) CiteSeer (b) MUTAG (c) IMDB-B (d) RDT-B

Figure 4: Ablation study to analyze the exponential partitioned similarity $\mathcal{S}_{part}$ and the semantics-consistency discriminator D.

B.4 Quantitative analysis

We conduct quantitative analyses to evaluate the effectiveness of the exponential partitioned similarity measure and the semantics-consistency discriminator in CaliGCL.

To assess the partitioned similarity measure, we train the GNN encoder with both the general contrastive loss and the partitioned contrastive loss. We then compare the distribution of positively-

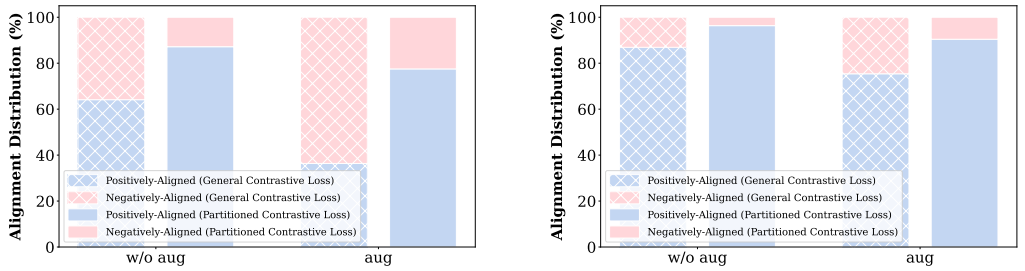

(a) IMDB-B (b) RDT-B

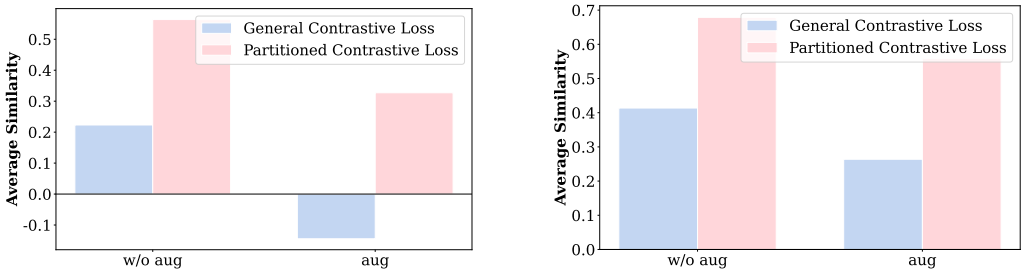

(c) IMDB-B (d) RDT-B

Figure 5: Quantitative analysis on similarity estimation bias, where "aug" means the data with augmentations and "w/o aug" means the data without augmentations.

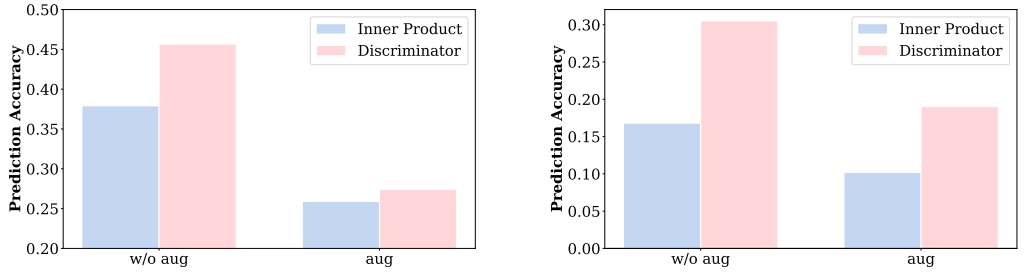

(a) IMDB-B (b) RDT-B

Figure 6: Quantitative analysis on semantic shift bias, where "aug" means the data with augmentations and "w/o aug" means the data without augmentations.

aligned and negatively-aligned partitions in Figure 7(a) and (b) on IMDB-B and RDT-B datasets, as well as the average similarity among positive pairs, which is defined as the total similarity divided by the number of positive pairs in Figure 7(c) and (d). The observed increases in the proportion of positively-aligned partitions and the average similarity clearly demonstrate that the partitioned contrastive loss effectively strengthens positively-synergistic features. Additionally, we compare the average similarity of positives with and without augmentations. Although random augmentations tend to reduce similarity among positives, the graph model using the exponential partitioned similarity still maintains good performance.

To evaluate the function of the semantics-consistency discriminator, we compare its prediction accuracy against similarity-based predictions. Specifically, we count the number of sample pairs predicted as positive pairs by the inner product and by the semantics-consistency discriminator (i.e., pairs with predicted consistency label $\tilde{l} = 1$), and compute their ratios over the ground-truth positives, respectively. As shown in Figure 6, the discriminator yields more accurate predictions, supporting its role in effectively calibrating the contrastive loss.

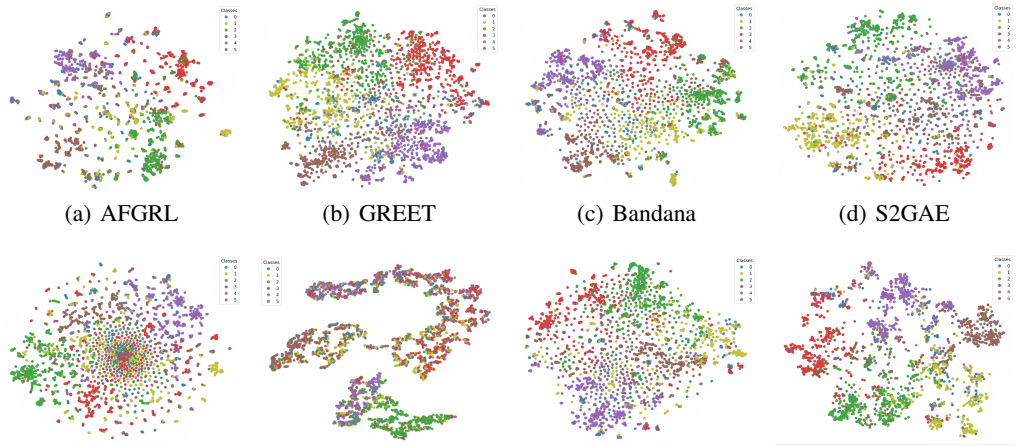

(a) AFGRL (b) GREET (c) Bandana (d) S2GAE

(e) iGCL (f) PiGCL (g) SGRL (h) CaliGCL

Figure 7: t-SNE visualization of CaliGCL and the comparative models on Citeseer dataset.

B.5 Visualization

We provide a t-SNE visualization comparing CaliGCL and other baselines to demonstrate the quality of learned representations. From the visualization results, we find the samples of different classes in PiGCL and iGCL are mixed; the boundaries of different classes in GREET, S2GAE, Bandana, and SGRL are ambiguous without margins. In contrast, the boundaries of different classes in CaliGCL are separated with larger margins.

B.6 Model complexity

We analyze the time and space complexity of CaliGCL by decomposing its key components: (1) Encoder forward pass. For an L-layer GNN such as GCN or GIN, the complexity of forward propagation is typically $\mathcal{O}(2L|\mathcal{E}|d)$, where $|\mathcal{E}|$ is the number of edges, d is the representation dimension. (2) Exponential partitioned similarity. For a batch of N nodes, computing similarities with all other N nodes has $\mathcal{O}(KN^2d)$ complexity. (3) Discriminator. For N^2 sample pairs, the total complexity is $\mathcal{O}(N^2Dd)$, where D is the dimension of the discriminator. Therefore, the complexity of CaliGCL is $\mathcal{O}(2L|\mathcal{E}|d + (K + D)N^2d)$.

B.7 Limitation

While the exponential partitioned similarity measure effectively enhances positively-synergistic features and suppresses negatively-synergistic ones, it remains a static mechanism that treats all partitions uniformly without explicitly distinguishing between aligned and misaligned components. A promising future direction would be to develop a learnable or attention-based partition weighting strategy that can automatically identify and emphasize positively-synergistic features while down-weighting negatively-synergistic ones in a data-driven manner.

NeurIPS Paper Checklist

1. **Claims**

   Question: Do the main claims made in the abstract and introduction accurately reflect the paper's contributions and scope?

   Answer: [Yes]

   Justification: In the abstract and introduction, we mention that graph contrastive learning models are limited by biases and propose a novel model, CaliGCL, to calibrate the biases.

   Guidelines:

   - The answer NA means that the abstract and introduction do not include the claims made in the paper.
   - The abstract and/or introduction should clearly state the claims made, including the contributions made in the paper and important assumptions and limitations. A No or NA answer to this question will not be perceived well by the reviewers.
   - The claims made should match theoretical and experimental results, and reflect how much the results can be expected to generalize to other settings.
   - It is fine to include aspirational goals as motivation as long as it is clear that these goals are not attained by the paper.

2. **Limitations**

   Question: Does the paper discuss the limitations of the work performed by the authors?

   Answer: [Yes]

   Justification: We have discussed the limitation in Appendix B.7.

   Guidelines:

   - The answer NA means that the paper has no limitation while the answer No means that the paper has limitations, but those are not discussed in the paper.
   - The authors are encouraged to create a separate "Limitations" section in their paper.
   - The paper should point out any strong assumptions and how robust the results are to violations of these assumptions (e.g., independence assumptions, noiseless settings, model well-specification, asymptotic approximations only holding locally). The authors should reflect on how these assumptions might be violated in practice and what the implications would be.
   - The authors should reflect on the scope of the claims made, e.g., if the approach was only tested on a few datasets or with a few runs. In general, empirical results often depend on implicit assumptions, which should be articulated.
   - The authors should reflect on the factors that influence the performance of the approach. For example, a facial recognition algorithm may perform poorly when image resolution is low or images are taken in low lighting. Or a speech-to-text system might not be used reliably to provide closed captions for online lectures because it fails to handle technical jargon.
   - The authors should discuss the computational efficiency of the proposed algorithms and how they scale with dataset size.
   - If applicable, the authors should discuss possible limitations of their approach to address problems of privacy and fairness.
   - While the authors might fear that complete honesty about limitations might be used by reviewers as grounds for rejection, a worse outcome might be that reviewers discover limitations that aren't acknowledged in the paper. The authors should use their best judgment and recognize that individual actions in favor of transparency play an important role in developing norms that preserve the integrity of the community. Reviewers will be specifically instructed to not penalize honesty concerning limitations.

3. **Theory assumptions and proofs**

   Question: For each theoretical result, does the paper provide the full set of assumptions and a complete (and correct) proof?

   Answer: [Yes]

Justification: We have provided some theoretical results based on assumptions in Section 3.

Guidelines:

- The answer NA means that the paper does not include theoretical results.
- All the theorems, formulas, and proofs in the paper should be numbered and cross-referenced.
- All assumptions should be clearly stated or referenced in the statement of any theorems.
- The proofs can either appear in the main paper or the supplemental material, but if they appear in the supplemental material, the authors are encouraged to provide a short proof sketch to provide intuition.
- Inversely, any informal proof provided in the core of the paper should be complemented by formal proofs provided in appendix or supplemental material.
- Theorems and Lemmas that the proof relies upon should be properly referenced.

4. **Experimental result reproducibility**

   Question: Does the paper fully disclose all the information needed to reproduce the main experimental results of the paper to the extent that it affects the main claims and/or conclusions of the paper (regardless of whether the code and data are provided or not)?

   Answer: [Yes]

   Justification: See Appendix B.

   Guidelines:

   - The answer NA means that the paper does not include experiments.
   - If the paper includes experiments, a No answer to this question will not be perceived well by the reviewers: Making the paper reproducible is important, regardless of whether the code and data are provided or not.
   - If the contribution is a dataset and/or model, the authors should describe the steps taken to make their results reproducible or verifiable.
   - Depending on the contribution, reproducibility can be accomplished in various ways. For example, if the contribution is a novel architecture, describing the architecture fully might suffice, or if the contribution is a specific model and empirical evaluation, it may be necessary to either make it possible for others to replicate the model with the same dataset, or provide access to the model. In general. releasing code and data is often one good way to accomplish this, but reproducibility can also be provided via detailed instructions for how to replicate the results, access to a hosted model (e.g., in the case of a large language model), releasing of a model checkpoint, or other means that are appropriate to the research performed.
   - While NeurIPS does not require releasing code, the conference does require all submissions to provide some reasonable avenue for reproducibility, which may depend on the nature of the contribution. For example
     (a) If the contribution is primarily a new algorithm, the paper should make it clear how to reproduce that algorithm.
     (b) If the contribution is primarily a new model architecture, the paper should describe the architecture clearly and fully.
     (c) If the contribution is a new model (e.g., a large language model), then there should either be a way to access this model for reproducing the results or a way to reproduce the model (e.g., with an open-source dataset or instructions for how to construct the dataset).
     (d) We recognize that reproducibility may be tricky in some cases, in which case authors are welcome to describe the particular way they provide for reproducibility. In the case of closed-source models, it may be that access to the model is limited in some way (e.g., to registered users), but it should be possible for other researchers to have some path to reproducing or verifying the results.

5. **Open access to data and code**

   Question: Does the paper provide open access to the data and code, with sufficient instructions to faithfully reproduce the main experimental results, as described in supplemental material?

Answer: [Yes]

Justification: We have provided the codes and example dataset in supplemental material.

Guidelines:

- The answer NA means that paper does not include experiments requiring code.
- Please see the NeurIPS code and data submission guidelines (`https://nips.cc/public/guides/CodeSubmissionPolicy`) for more details.
- While we encourage the release of code and data, we understand that this might not be possible, so "No" is an acceptable answer. Papers cannot be rejected simply for not including code, unless this is central to the contribution (e.g., for a new open-source benchmark).
- The instructions should contain the exact command and environment needed to run to reproduce the results. See the NeurIPS code and data submission guidelines (`https://nips.cc/public/guides/CodeSubmissionPolicy`) for more details.
- The authors should provide instructions on data access and preparation, including how to access the raw data, preprocessed data, intermediate data, and generated data, etc.
- The authors should provide scripts to reproduce all experimental results for the new proposed method and baselines. If only a subset of experiments are reproducible, they should state which ones are omitted from the script and why.
- At submission time, to preserve anonymity, the authors should release anonymized versions (if applicable).
- Providing as much information as possible in supplemental material (appended to the paper) is recommended, but including URLs to data and code is permitted.

6. **Experimental setting/details**

   Question: Does the paper specify all the training and test details (e.g., data splits, hyperparameters, how they were chosen, type of optimizer, etc.) necessary to understand the results?

   Answer: [Yes]

   Justification: See Section 4 and Appendix B.

   Guidelines:

   - The answer NA means that the paper does not include experiments.
   - The experimental setting should be presented in the core of the paper to a level of detail that is necessary to appreciate the results and make sense of them.
   - The full details can be provided either with the code, in appendix, or as supplemental material.

7. **Experiment statistical significance**

   Question: Does the paper report error bars suitably and correctly defined or other appropriate information about the statistical significance of the experiments?

   Answer: [Yes]

   Justification: See Table 1 and Table 2 in Section 4.

   Guidelines:

   - The answer NA means that the paper does not include experiments.
   - The authors should answer "Yes" if the results are accompanied by error bars, confidence intervals, or statistical significance tests, at least for the experiments that support the main claims of the paper.
   - The factors of variability that the error bars are capturing should be clearly stated (for example, train/test split, initialization, random drawing of some parameter, or overall run with given experimental conditions).
   - The method for calculating the error bars should be explained (closed form formula, call to a library function, bootstrap, etc.)
   - The assumptions made should be given (e.g., Normally distributed errors).
   - It should be clear whether the error bar is the standard deviation or the standard error of the mean.

- It is OK to report 1-sigma error bars, but one should state it. The authors should preferably report a 2-sigma error bar than state that they have a 96% CI, if the hypothesis of Normality of errors is not verified.
- For asymmetric distributions, the authors should be careful not to show in tables or figures symmetric error bars that would yield results that are out of range (e.g. negative error rates).
- If error bars are reported in tables or plots, The authors should explain in the text how they were calculated and reference the corresponding figures or tables in the text.

8. **Experiments compute resources**

   Question: For each experiment, does the paper provide sufficient information on the computer resources (type of compute workers, memory, time of execution) needed to reproduce the experiments?

   Answer: [Yes]

   Justification: See Section 4.

   Guidelines:

   - The answer NA means that the paper does not include experiments.
   - The paper should indicate the type of compute workers CPU or GPU, internal cluster, or cloud provider, including relevant memory and storage.
   - The paper should provide the amount of compute required for each of the individual experimental runs as well as estimate the total compute.
   - The paper should disclose whether the full research project required more compute than the experiments reported in the paper (e.g., preliminary or failed experiments that didn't make it into the paper).

9. **Code of ethics**

   Question: Does the research conducted in the paper conform, in every respect, with the NeurIPS Code of Ethics `https://neurips.cc/public/EthicsGuidelines`?

   Answer: [Yes]

   Justification: I have read the NeurIPS Code of Ethics `https://neurips.cc/public/EthicsGuidelines`, and the research conducted in the paper conforms to the NeurIPS Code of Ethics.

   Guidelines:

   - The answer NA means that the authors have not reviewed the NeurIPS Code of Ethics.
   - If the authors answer No, they should explain the special circumstances that require a deviation from the Code of Ethics.
   - The authors should make sure to preserve anonymity (e.g., if there is a special consideration due to laws or regulations in their jurisdiction).

10. **Broader impacts**

    Question: Does the paper discuss both potential positive societal impacts and negative societal impacts of the work performed?

    Answer: [NA]

    Justification: Due to the nature of this work, there is no negative societal impact of the work performed.

    Guidelines:

    - The answer NA means that there is no societal impact of the work performed.
    - If the authors answer NA or No, they should explain why their work has no societal impact or why the paper does not address societal impact.
    - Examples of negative societal impacts include potential malicious or unintended uses (e.g., disinformation, generating fake profiles, surveillance), fairness considerations (e.g., deployment of technologies that could make decisions that unfairly impact specific groups), privacy considerations, and security considerations.

- The conference expects that many papers will be foundational research and not tied to particular applications, let alone deployments. However, if there is a direct path to any negative applications, the authors should point it out. For example, it is legitimate to point out that an improvement in the quality of generative models could be used to generate deepfakes for disinformation. On the other hand, it is not needed to point out that a generic algorithm for optimizing neural networks could enable people to train models that generate Deepfakes faster.
- The authors should consider possible harms that could arise when the technology is being used as intended and functioning correctly, harms that could arise when the technology is being used as intended but gives incorrect results, and harms following from (intentional or unintentional) misuse of the technology.
- If there are negative societal impacts, the authors could also discuss possible mitigation strategies (e.g., gated release of models, providing defenses in addition to attacks, mechanisms for monitoring misuse, mechanisms to monitor how a system learns from feedback over time, improving the efficiency and accessibility of ML).

11. **Safeguards**

    Question: Does the paper describe safeguards that have been put in place for responsible release of data or models that have a high risk for misuse (e.g., pretrained language models, image generators, or scraped datasets)?

    Answer: [NA]

    Justification: Our research dosen't pose such risks.

    Guidelines:

    - The answer NA means that the paper poses no such risks.
    - Released models that have a high risk for misuse or dual-use should be released with necessary safeguards to allow for controlled use of the model, for example by requiring that users adhere to usage guidelines or restrictions to access the model or implementing safety filters.
    - Datasets that have been scraped from the Internet could pose safety risks. The authors should describe how they avoided releasing unsafe images.
    - We recognize that providing effective safeguards is challenging, and many papers do not require this, but we encourage authors to take this into account and make a best faith effort.

12. **Licenses for existing assets**

    Question: Are the creators or original owners of assets (e.g., code, data, models), used in the paper, properly credited and are the license and terms of use explicitly mentioned and properly respected?

    Answer: [Yes]

    Justification: We have cited the original paper that produced the code package or dataset.

    Guidelines:

    - The answer NA means that the paper does not use existing assets.
    - The authors should cite the original paper that produced the code package or dataset.
    - The authors should state which version of the asset is used and, if possible, include a URL.
    - The name of the license (e.g., CC-BY 4.0) should be included for each asset.
    - For scraped data from a particular source (e.g., website), the copyright and terms of service of that source should be provided.
    - If assets are released, the license, copyright information, and terms of use in the package should be provided. For popular datasets, `paperswithcode.com/datasets` has curated licenses for some datasets. Their licensing guide can help determine the license of a dataset.
    - For existing datasets that are re-packaged, both the original license and the license of the derived asset (if it has changed) should be provided.

- If this information is not available online, the authors are encouraged to reach out to the asset's creators.

13. **New assets**

    Question: Are new assets introduced in the paper well documented and is the documentation provided alongside the assets?

    Answer: [NA]

    Justification: The paper does not release new assets.

    Guidelines:

    - The answer NA means that the paper does not release new assets.
    - Researchers should communicate the details of the dataset/code/model as part of their submissions via structured templates. This includes details about training, license, limitations, etc.
    - The paper should discuss whether and how consent was obtained from people whose asset is used.
    - At submission time, remember to anonymize your assets (if applicable). You can either create an anonymized URL or include an anonymized zip file.

14. **Crowdsourcing and research with human subjects**

    Question: For crowdsourcing experiments and research with human subjects, does the paper include the full text of instructions given to participants and screenshots, if applicable, as well as details about compensation (if any)?

    Answer: [NA]

    Justification: The paper does not involve crowdsourcing nor research with human subjects.

    Guidelines:

    - The answer NA means that the paper does not involve crowdsourcing nor research with human subjects.
    - Including this information in the supplemental material is fine, but if the main contribution of the paper involves human subjects, then as much detail as possible should be included in the main paper.
    - According to the NeurIPS Code of Ethics, workers involved in data collection, curation, or other labor should be paid at least the minimum wage in the country of the data collector.

15. **Institutional review board (IRB) approvals or equivalent for research with human subjects**

    Question: Does the paper describe potential risks incurred by study participants, whether such risks were disclosed to the subjects, and whether Institutional Review Board (IRB) approvals (or an equivalent approval/review based on the requirements of your country or institution) were obtained?

    Answer: [NA]

    Justification: The paper does not involve crowdsourcing nor research with human subjects.

    Guidelines:

    - The answer NA means that the paper does not involve crowdsourcing nor research with human subjects.
    - Depending on the country in which research is conducted, IRB approval (or equivalent) may be required for any human subjects research. If you obtained IRB approval, you should clearly state this in the paper.
    - We recognize that the procedures for this may vary significantly between institutions and locations, and we expect authors to adhere to the NeurIPS Code of Ethics and the guidelines for their institution.
    - For initial submissions, do not include any information that would break anonymity (if applicable), such as the institution conducting the review.

16. **Declaration of LLM usage**

Question: Does the paper describe the usage of LLMs if it is an important, original, or non-standard component of the core methods in this research? Note that if the LLM is used only for writing, editing, or formatting purposes and does not impact the core methodology, scientific rigorousness, or originality of the research, declaration is not required.

Answer: [NA]

Justification: LLMs are used only for writing, editing, or formatting purposes in this paper, but do not serve as any important, original, or non-standard components.

Guidelines:

- The answer NA means that the core method development in this research does not involve LLMs as any important, original, or non-standard components.
- Please refer to our LLM policy (`https://neurips.cc/Conferences/2025/LLM`) for what should or should not be described.